

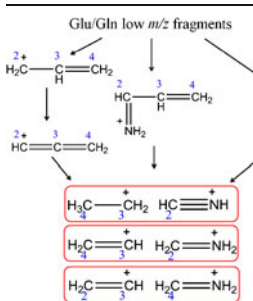
Low Mass MS/MS Fragments of Protonated Amino Acids Used for Distinction of Their ^{13}C -Isotopomers in Metabolic Studies

Xin Ma,^{1,2} Shai Dagan,^{1,3} Árpád Somogyi,¹ Vicki H. Wysocki,^{1,2} Patricia Y. Scaraffia¹

¹Department of Chemistry and Biochemistry, The University of Arizona, Tucson, AZ 85721, USA

²Department of Chemistry and Biochemistry, The Ohio State University, Columbus, OH 43210, USA

³Israel Institute for Biological Research, Ness Ziona, 74100, Israel



Abstract. Glu, Gln, Pro, and Ala are the main amino acids involved in ammonia detoxification in mosquitoes. In order to develop a tandem mass spectrometry method (MS^2) to monitor each carbon of the above isotopically-labeled ^{13}C -amino acids for metabolic studies, the compositions and origins of atoms in fragments of the protonated amino acid should be first elucidated. Thus, various electrospray (ESI)-based MS^2 tools were employed to study the fragmentation of these unlabeled and isotopically-labeled amino acids and better understand their dissociation pathways. A broad range of fragments, including previously-undescribed low m/z fragments was revealed. The formulae of the fragments (from m/z 130 down to m/z 27) were confirmed by their accurate masses. The

structures and conformations of the larger fragments of Glu were also explored by ion mobility mass spectrometry (IM-MS) and gas-phase hydrogen/deuterium exchange (HDX) experiments. It was found that some low m/z fragments (m/z 27–30) are common to Glu, Gln, Pro, and Ala. The origins of carbons in these small fragments are discussed and additional collision induced dissociation (CID) MS^2 fragmentation pathways are proposed for them. It was also found that small fragments ($\leq m/z$ 84) of protonated, methylated Glu, and methylated Gln are the same as those of the underivatized Glu and Gln. Taken together, the new approach of utilizing low m/z fragments can be applied to distinguish, identify, and quantify ^{13}C -amino acids labeled at various positions, either in the backbone or side chain.

Key words: Low m/z fragments, ^{13}C -amino acids, ESI, CID MS^2 , FTICR, IM-MS, Q-TOF

Received: 10 October 2012/Revised: 10 December 2012/Accepted: 13 December 2012/Published online: 27 February 2013

Introduction

Stable isotopes such as ^{15}N and ^{13}C are widely used as tracers to monitor and quantify metabolic pathways in humans as well as other organisms. Usually, isotopically-labeled compounds are introduced into a biological system and the fluxes of these stable isotopes can then be quantified to provide accurate information about different metabolic processes [1–5]. The common techniques to monitor and quantify these labeled compounds in complex metabolic networks are nuclear magnetic resonance (NMR) spectroscopy, gas chromatography mass spectrometry (GC-MS), and

direct infusion electrospray (ESI) MS^2 [6–20]. Jeffrey et al. [16] compared the performance of NMR, GC-MS (Electron Ionization-EI) and GC- MS^2 in the analysis of isotopically-labeled Glu in the citric acid cycle. The authors concluded that MS^2 and NMR are comparable, whereas the full-scan EI-MS is the least accurate technique [16]. Accurate mass measurements by Fourier transform ion cyclotron resonance (FTICR) MS also show potential to be a useful tool to monitor ^{13}C distribution in amino acids, based on the exact mass shifts of ^{13}C labeled precursor ions and fragments [10, 11, 20].

In our laboratory, we have applied ESI- MS^2 for studying the ammonia metabolism in *Aedes aegypti* mosquitoes, the main vectors of dengue and yellow fever. By feeding *A. aegypti* females with isotopically-labeled ^{15}N -compounds (such as $^{15}\text{NH}_4\text{Cl}$), we discovered that mosquitoes have an extraordinary biochemical machine to efficiently detoxify ammonia. Indeed, they synthesize specific amino acids and excrete several nitrogen wastes through multiple metabolic

Electronic supplementary material The online version of this article (doi:10.1007/s13361-012-0574-9) contains supplementary material, which is available to authorized users.

Correspondence to: Patricia Y. Scaraffia; e-mail: scaraffi@email.arizona.edu

pathways [6–9]. By using this strategy, female mosquitoes are able to survive toxic ammonia concentrations released during the digestion of a blood meal. To better understand this complex metabolic process and to identify possible targets that can be utilized for controlling mosquito populations, we are now interested in investigating the carbon metabolism of Glu, Gln, Pro, and Ala, the main amino acids involved in ammonia detoxification in *A. aegypti*. In order to monitor the carbons of isotopically-labeled amino acids by ESI-MS², there must be fragments from one or more fragmentation events that can be used to separately identify each carbon. Towards this goal, we first studied the compositions and origins of the atoms in fragments of the protonated amino acids. It has been reported that the carboxylic acid groups dissociate from protonated amino acids at low collision energies (CE) in collision induced dissociation (CID) [21]. For example, protonated Glu (m/z 148) is reported to lose two CH_2O_2 units to produce the m/z 56 fragment [21–24], and this fragment is used for quantification of [$1\text{-}^{13}\text{C}$]-Glu and [$5\text{-}^{13}\text{C}$]-Glu [14, 15]. The fragmentation of protonated Gln (m/z 147) is reported to be similar to that of protonated Glu [21–24]. It was also reported that protonated Pro (m/z 116) and Ala (m/z 90) lose CH_2O_2 to form m/z 70 (Pro fragment) and 44 (Ala fragment) peaks [21]. However, these relatively large fragments can only be used to distinguish, identify and quantify the carbons of the carboxylic acid groups. In order to monitor each carbon in Glu, as well as the other amino acids, understanding of the compositions and origins of the carbons in smaller fragments is required.

Here, we further explore and extend the range of fragments of protonated Glu (m/z 148), Gln (m/z 147), Pro (m/z 116), and Ala (m/z 90) all the way down to m/z 27. Glu is studied in detail and presented as a representative example for the other amino acids. FTICR and quadrupole time of flight (Q-TOF) mass spectrometry methods were employed to measure the accurate masses of the fragments and reveal their chemical formulae. Also, the origins of the carbons in the fragments were elucidated based on the mass shifts of the fragments in the isotopically-labeled amino acids. Gas-phase hydrogen/deuterium exchange (HDX) and ion mobility mass spectrometry (IM-MS) were also used to explore the possible configurations of some of the fragments. Based on these results, a CID MS² pathway map from the precursor, all the way to the m/z 27 fragment of protonated Glu, is proposed. Some of the low m/z fragments (m/z 27–30), found in protonated Glu, are also observed in the protonated Gln, Pro and Ala. The origins of the carbons of these small fragments are discussed.

Experimental

Chemicals and Reagents

Unlabeled amino acids, Glu-dimethyl-ester, trimethylsilyldiazomethane, formic acid, ND_3 , and [$3\text{-}^{13}\text{C}$]-Glu were

purchased from Sigma-Aldrich (St. Louis, MO, USA). [$5\text{-}^{13}\text{C}$]-Glu was obtained from Santa Cruz Biotechnology, Inc. (San Diego, CA, USA). [$4\text{-}^{13}\text{C}$]-Gln and [$4\text{-}^{13}\text{C}$]-Glu were generously provided by Dr. Kanamatsu (Soka University, Tokyo, Japan) and Dr. Takatori (Meiji Pharmaceutical University, Tokyo, Japan) respectively. [^{15}N]-Glu, [$1,2\text{-}^{13}\text{C}$]-Glu, [$^{13}\text{C}_5\text{ }^{15}\text{N}$]-Glu, [$2\text{-}^{15}\text{N}$]-Gln, [$5\text{-}^{15}\text{N}$]-Gln, [$2,5\text{-}^{15}\text{N}_2$]-Gln, [$1,2\text{-}^{13}\text{C}$]-Gln, [$3\text{-}^{13}\text{C}$]-Gln, [$^{13}\text{C}_5\text{ }^{15}\text{N}_2$]-Gln, [^{15}N]-Pro, [$1\text{-}^{13}\text{C}$]-Pro, [$^{13}\text{C}_5\text{ }^{15}\text{N}$]-Pro, [^{15}N]-Ala, [$1\text{-}^{13}\text{C}$]-Ala, [$2\text{-}^{13}\text{C}$]-Ala, and [$3\text{-}^{13}\text{C}$]-Ala were purchased from Cambridge Isotope Laboratories (Andover, MA, USA). LC/MS grade water was purchased from Mallinckrodt Baker Inc. (Phillipsburg, NJ, USA). HPLC grade methanol and acetonitrile were purchased from EMD Chemicals Inc. (Gibbstown, NJ, USA).

Amino Acid Derivatization

For some experiments, the amino acids were methylated by a method described previously with some modifications [25]. Briefly, 50 nmol of each amino acid was dissolved in 3 mL acetone/methanol (70/30 vol/vol). Ten μL of 2 M trimethylsilyldiazomethane was added into the solution dropwise and stirred for 4 h. The solvents were removed under a stream of N_2 gas.

Low Resolution Tandem Mass Spectrometry

Low resolution MS² was performed using ESI/triple quadrupole (QqQ) mass spectrometers (AB/SCIEX 4000 QTRAP and AB/SCIEX 3000 QqQ; Foster City, CA, USA) in the positive ion mode. The spray solvent utilized was a methanol-water-formic acid mixture (70:30:0.1 vol/vol/vol). Several unlabeled and isotopically-labeled amino acid solutions at 0.5–10 μM were introduced into the ESI source by infusion at a flow rate of 7 $\mu\text{L}/\text{min}$. The ESI capillary voltage utilized was 5 kV and the source temperature was 250 °C. Nitrogen served as the collision gas (8 mTorr). A laboratory collision energy of 15–55 eV was applied to dissociate the ions to various degrees. To perform MS³ experiments, the declustering potential was set to 80 V to in-source dissociate the precursor, while the precursor fragment was selected in the first quadrupole and CID was used to further dissociate it.

Fourier Transform Ion Cyclotron Resonance (FTICR) Mass Spectrometry

High resolution MS² and gas-phase HDX experiments were performed in an ESI/FTICR (Bruker APEX Qh 9.4T, Billerica, MA, USA) mass spectrometer in the positive ion mode. The FTICR instrument was externally calibrated for the low m/z region and the measured masses are reported with a four decimal accuracy and compared with theoretical (calculated) values using the Bruker data processing software. The spray solvent utilized was a water-acetonitrile-formic acid mixture (50:50:0.1 vol/vol/vol). Unlabeled and

isotopically-labeled amino acid solutions (10 μM) were infused into the ESI source with a flow rate of 2.5 $\mu\text{L}/\text{min}$. The capillary voltage was 4.8 kV, the spray shield was 3.3 kV, and the source temperature was 200 $^{\circ}\text{C}$. Sustained off-resonance irradiation (SORI)-CID was used to dissociate the ions. The argon pressure measured at the FTICR cell was $\sim 3 \times 10^{-8}$ mbar. The SORI power was typically 1 %–2 % with a pulse duration of 100 ms and frequency offset of 500 Hz. Gas-phase HDX experiments were performed with ND_3 . The ND_3 pressure was ~ 0.8 mbar and the reaction time in the FTICR cell varied between 0.1 and 10 s.

Electrospray Quadrupole-Time of Flight (Q-TOF) Ion Mobility Mass Spectrometry (ESI-IM-MS)

IM-MS and accurate mass measurements were performed using an ESI/quadrupole/IM/TOF mass spectrometer (Waters, SYNAPT G2, Manchester, UK) in the positive ion mode. The calibration was performed for the low mass range. The concentration of amino acid solutions was 0.1 mM and the sample flow rate was set to be 5 $\mu\text{L}/\text{min}$. The ESI capillary voltage was 3 kV and the source temperature was 260 $^{\circ}\text{C}$. Argon (3×10^{-2} mbar) was used as the collision gas and the CE was 10–15 eV. The drift times of amino acid fragments were measured in the “ion mobility” mode. The pressure of nitrogen in the ion mobility chamber was ~ 2.2 mbar. The ion mobility spectrometry (IMS) wave height and velocity were optimized at 16.0 V and 1500 ms^{-1} . Accurate mass measurements were performed in the TOF “resolution” mode.

Results and Discussion

Low and High Energy Collision Induced Dissociation (CID) of Protonated Glu and Isotopically-Labeled Glu

In order to develop a method to monitor each possible ^{13}C carbon in Glu, several different Glu isotopomers were used. Figure 1 shows the QqQ MS^2 spectra of Glu + H^+ (m/z 148 precursor), ^{15}N – Glu + H^+ (m/z 149), $[1,2-^{13}\text{C}]$ – Glu + H^+ (m/z 150), $[3-^{13}\text{C}]$ – Glu + H^+ (m/z 149), $[4-^{13}\text{C}]$ – Glu + H^+ (m/z 149), $[5-^{13}\text{C}]$ – Glu + H^+ (m/z 149), and $^{13}\text{C}_5^{15}\text{N}$ – Glu + H^+ (m/z 154) (refer to Scheme 1 for numbering of atoms). The MS^2 spectra exhibit m/z 130, 102, and 84 peaks or their analogs in the labeled compounds at 15 eV collision energy (blue spectra in Figure 1). This is in agreement with previous studies performed with unlabeled Glu [21–24]. The m/z 130 peak results from a loss of neutral water, whereas m/z 102 peak results from a 46 Da neutral loss (CH_2O_2) [22–24]. In the MS^2 spectrum of ^{15}N – Glu + H^+ (Figure 1c), the neutral loss is also 46 Da indicating that the nitrogen is not lost. Because carbon number 1 (C1) is lost, the m/z 102 peak shifts up by only one Da in the $[1,2-^{13}\text{C}]$ – Glu + H^+ spectrum (Figure 1e). This conclusion is further confirmed by the spectra of $[3-^{13}\text{C}]$ – Glu + H^+ , $[4-^{13}\text{C}]$ – Glu + H^+ ,

and $[5-^{13}\text{C}]$ – Glu + H^+ (Figure 1g, 1i, and 1k, respectively). The m/z 103 peaks in these spectra show that C3, C4, and C5 carbons remain in this fragment, with C1 lost. In the $^{13}\text{C}_5^{15}\text{N}$ – Glu (Figure 1m), the neutral loss is 47 Da, confirming that only one carbon is in the neutral lost.

One of the major fragments observed at 15 eV collision energy is the m/z 84 peak (Figure 1a), which is the result of the 64 Da neutral loss (two water molecules and one carbon monoxide) from Glu + H^+ [10, 11, 21–24]. In the spectrum of ^{15}N – Glu + H^+ (Figure 1c), the m/z 84 peak shifts up by one Da, indicating that the nitrogen is part of this fragment. The carbon monoxide loss to form the m/z 84 peak also contains C1. As a result, in the spectrum of $[1,2-^{13}\text{C}]$ – Glu + H^+ (Figure 1e), the m/z 84 peak shifts up by only one Da, which is also true for the spectra of $[3-^{13}\text{C}]$ – Glu + H^+ , $[4-^{13}\text{C}]$ – Glu + H^+ and $[5-^{13}\text{C}]$ – Glu + H^+ (Figure 1g, 1i, and 1k, respectively). In the spectrum of $^{13}\text{C}_5^{15}\text{N}$ – Glu + H^+ (Figure 1m), the m/z 84 peak, containing one nitrogen and four carbons, shifts up by five Da, in agreement with previous studies that show that C1 dissociates from protonated Glu first, followed by dissociation of C5 [10, 11, 21–24].

ESI fragments smaller than m/z 56 were not reported previously. The compositions of smaller fragments may provide specific and useful information to separately monitor each ^{13}C -carbon in Glu and other amino acids. To further dissociate and explore smaller products of Glu + H^+ , a higher CID collision energy (55 eV, red spectra in Figure 1) was applied. High energy MS^2 experiments provided low m/z fragments with higher intensity than various MS^3 experiments. At this higher CE, the dominant peak is m/z 56, and the neutral loss from the precursor is 92 Da, which results from two water and two carbon monoxide molecules. The two carbon monoxide molecules contain the C1 and C5 carbons of the carboxyl groups, which are easier to dissociate from Glu + H^+ [10, 11]. The m/z 56 peak shifts up by one Da in the MS^2 spectrum of ^{15}N – Glu + H^+ (Figure 1c), indicating that the nitrogen is in this fragment. In the spectra of $[1,2-^{13}\text{C}]$ – Glu + H^+ , $[3-^{13}\text{C}]$ – Glu + H^+ , $[4-^{13}\text{C}]$ – Glu + H^+ (Figure 1e, 1g, and 1i, respectively), this peak also shifts up by one Da, suggesting that C1 is involved in the neutral loss. The other carbon monoxide contains C5 as the m/z 56 peak does not shift in the spectrum of $[5-^{13}\text{C}]$ – Glu + H^+ (Figure 1k).

A m/z 41 peak was also observed at 55 eV CID (Figure 1a). Our data suggest that this peak results from CONH loss (43 Da loss) from the m/z 84 peak, and not from the m/z 56 fragment, as is discussed below. The MS^2 spectrum of ^{15}N – Glu + H^+ (Figure 1c) indicates that the nitrogen is in the neutral loss group (CO^{15}NH) because the m/z 41 fragment does not shift. In correlation with these data, the spectrum of $^{13}\text{C}_5^{15}\text{N}$ – Glu + H^+ (Figure 1m) gives a neutral loss from m/z 89 of 45 Da, corresponding to $^{13}\text{CO}^{15}\text{NH}$, whereas in the $[1,2-^{13}\text{C}]$ – Glu + H^+ , $[3-^{13}\text{C}]$ – Glu + H^+ and $[4-^{13}\text{C}]$ – Glu + H^+ (Figure 1e, 1g, and 1i, respectively) this neutral loss is 43 Da (CONH). In the $[5-^{13}\text{C}]$ – Glu + H^+

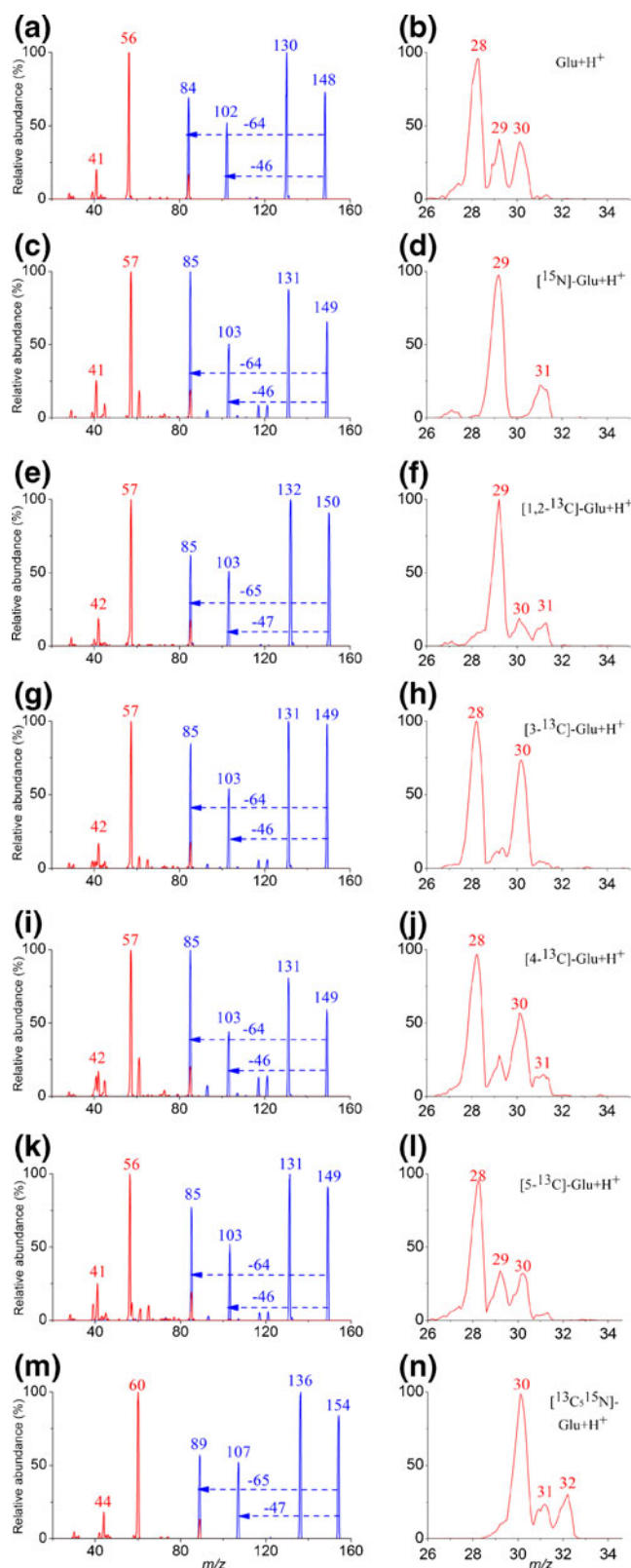
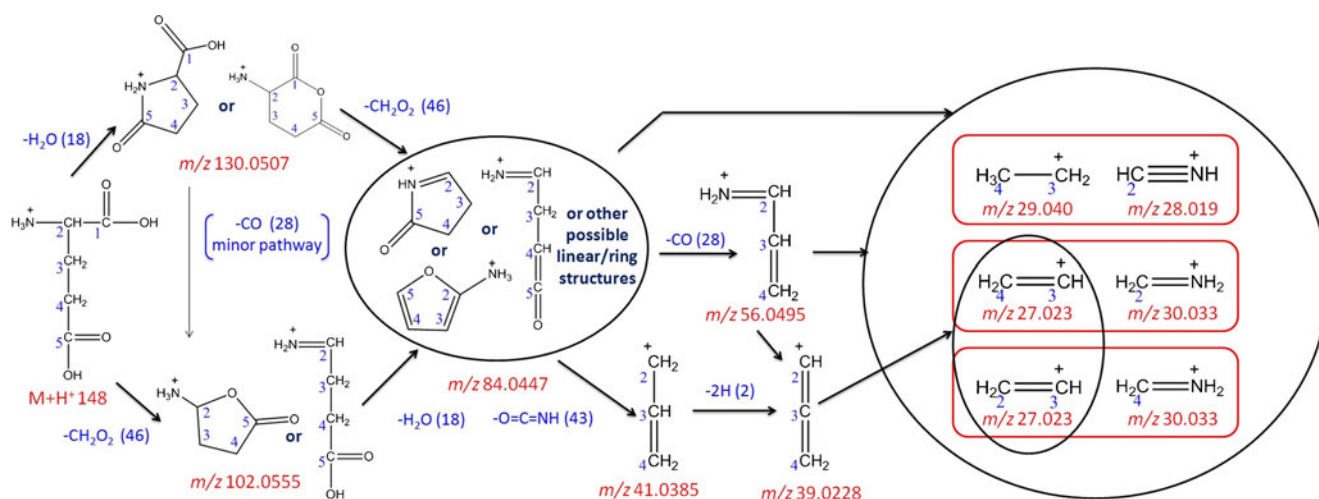


Figure 1. MS^2 of protonated Glu and isotopically-labeled Glu performed on a QqQ instrument in the product ion scan mode. **(a)** Glu + H^+ (m/z 148); **(c)** ^{15}N – Glu + H^+ (m/z 149); **(e)** $[1,2-^{13}\text{C}]$ – Glu + H^+ (m/z 150); **(g)** $[3-^{13}\text{C}]$ – Glu + H^+ (m/z 149); **(i)** $[4-^{13}\text{C}]$ – Glu + H^+ (m/z 149); **(k)** $[5-^{13}\text{C}]$ – Glu + H^+ (m/z 149); **(m)** $[^{13}\text{C}_5^{15}\text{N}]$ – Glu + H^+ (m/z 154). On the left (**a, c, e, g, i, k, and m**), superimposed spectra are shown, obtained at a CE of 15 eV (blue) and 55 eV (red). On the right (**b, d, f, h, j, l, and n**), blow-ups of the low m/z region (m/z 26–35, CE 55 eV) are shown by magnifying 20 to 100 times. The spectra are normalized to the highest peak in each m/z range



Scheme 1. Proposed CID MS² fragmentation pathways, ion structures* and origins of carbons of Glu. The accurate masses of the large fragments are measured by FTICR and those of the small fragments ($\leq m/z$ 30) are measured by Q-TOF. The thinner arrow from m/z 130 to m/z 102 represents a minor pathway. The fragments in the circle on the right are from the m/z 56 and m/z 84 fragments. The m/z 41 and m/z 39 fragments may also form the m/z 27 fragment, although *via* high energy reactions. The fragments in each red box make a pair of charge-competing products. Structures of fragments $\geq m/z$ 84 were proposed previously [10, 11, 22–24]. (*For simplicity not all possible isomeric ion structures are indicated)

(Figure 1k), the neutral loss is 44 Da ($^{13}\text{CONH}$) showing that the carbon in the leaving group is C5.

In the m/z 27–32 range, several small peaks were observed in the MS² spectrum of Glu at a collision energy of 55 eV (Figure 1b). The m/z 28 and 30 fragments contain nitrogen as these two peaks shift up by one Da in the spectrum of [^{15}N] – Glu + H⁺ (Figure 1d). In contrast, the m/z 29 peak does not shift in the spectrum of [^{15}N] – Glu + H⁺ (Figure 1d), indicating that this fragment does not contain nitrogen. The m/z 28 and 30 fragments also contain C2 because they shift up by one Da in the spectrum of [1,2- ^{13}C] – Glu + H⁺ (Figure 1f). It is known from the literature that C1 is the first to leave [21–24], and therefore m/z 28 must contain C2 and not C1. In the spectrum of [3- ^{13}C] – Glu + H⁺, [4- ^{13}C] – Glu + H⁺ and [5- ^{13}C] – Glu + H⁺ (Figure 1h, j, and l, respectively), the m/z 28 and m/z 30 peaks do not shift, confirming that these fragments contain C2. Based on the information above, the formula of the m/z 28 peak corresponds to CH₂N whereas the formula of the m/z 30 peak corresponds to CH₄N. In [$^{13}\text{C}_5$ ^{15}N] – Glu + H⁺ (Figure 1n), all three peaks, including m/z 29, shift up by two Da, suggesting that the m/z 29 peak contains two carbons. Therefore, the proposed formula for this peak is C₂H₅. Because shifted peaks may overlap with other peaks, high resolution, accurate mass measurements of these fragments are required to further explore and discuss the origins of the carbons.

Accurate masses of the fragments, from m/z 130 down to m/z 30, were measured by FTICR-MS and their formulae were confirmed (Table 1a). Because of the difficulty in detecting fragments $\leq m/z$ 30 in FTICR, the Q-TOF was employed to explore the composition and origin of the carbons of the smaller fragments (m/z 27–32) of protonated

Glu and isotopically-labeled Glu (Figure 2 and Table 1b). The spectra of Glu + H⁺ (Figure 2a) and [5- ^{13}C] – Glu + H⁺ (Figure 2e) in this m/z range are exactly the same, indicating the fragments in this m/z range do not contain C5. In the spectrum of Glu + H⁺, the m/z 28.019 peak is dominant (Figure 2a) and its accurate mass corresponds to CH₂N. In the spectrum of [1,2- ^{13}C] – Glu + H⁺ (Figure 2b), the peak shifts to m/z 29.021 ($^{13}\text{CH}_2\text{N}$), indicating this fragment contains either C1 or C2. Because C1 is in the carboxylic acid group, it dissociated from Glu at a low CE [10, 11, 22–24]. The carbon in the m/z 28.019 peak is therefore most likely C2. The m/z 30.033 (CH₄N) fragment also contains nitrogen and carbon. However, only about half of the m/z 30.033 peak population shifts to m/z 31.037 ($^{13}\text{CH}_4\text{N}$) in the spectrum of [1,2- ^{13}C] – Glu + H⁺ (Figure 2b). The other half shifted to m/z 31.037 ($^{13}\text{CH}_4\text{N}$) in the spectrum of [4- ^{13}C] – Glu + H⁺ (Figure 2d), but there was no shift in the spectrum of [3- ^{13}C] – Glu + H⁺ (Figure 2c), indicating that the CH₄N peak at m/z 30.033 peak is a mixture implies either C2 or C4. This difference between the m/z 28.019 and m/z 30.033 labeled fragments indicates that there are separate pathways to form each of these two fragments. Thus, there is most likely more than one pathway involving different carbons to form CH₄N (Scheme 1). One of these pathways presumably involves a rearrangement to combine C4 and the nitrogen.

Another major peak in the m/z 27–32 range is at m/z 29.040, which corresponds to C₂H₅. This peak does not shift in the spectrum of [1,2- ^{13}C] – Glu + H⁺ (Figure 2b), indicating that this fragment contains neither C1 nor C2. As discussed previously, the low m/z fragments do not contain C5, thus it is likely that the carbons in this m/z 29 fragment are C3 and C4. The spectra of [3- ^{13}C] – Glu + H⁺ and [4- ^{13}C] – Glu + H⁺ (Figure 2c, d) confirm this hypothesis.

Table 1. Accurate masses of Glu + H^+ fragments measured by (a) FTICR; (b) Q-TOF

(a)			
Proposed formula	Theoretical mass (Da)	Experimental mass (Da)	Error (ppm)
$\text{C}_5\text{H}_8\text{NO}_3$	130.0499	130.0507	+6.1
$\text{C}_4\text{H}_8\text{NO}_2$	102.0550	102.0555	+4.8
$\text{C}_4\text{H}_6\text{NO}$	84.0444	84.0447	+3.5
$\text{C}_3\text{H}_6\text{N}$	56.0495	56.0495	+0.0
C_3H_5	41.0386	41.0385	-2.4
C_3H_3	39.0229	39.0228	-2.5
CH_4N	30.0338	30.0337	-3.3
(b)			
Proposed formula	Theoretical mass (Da)	Experimental mass (Da)	Δ (Da)
CH_4N	30.034	30.033	-0.001
C_2H_5	29.039	29.040	+0.001
CH_2N	28.018	28.019	+0.001
C_2H_3	27.023	27.023	+0.000
$^{13}\text{CH}_4\text{N}$	31.037	31.037	+0.000
$^{13}\text{CCH}_5$	30.042	30.043	+0.001
$^{13}\text{CH}_2\text{N}$	29.021	29.021	+0.000
$^{13}\text{CCH}_3$	28.026	28.026	+0.000

The m/z 29.040 (C_2H_5) peak completely shifts to m/z 30.043 ($^{13}\text{CCH}_5$) in both of these spectra. This C_2H_5 and the CH_2N fragments could both originate from the m/z 56 ($\text{C}_3\text{H}_6\text{N}$) fragment.

Unlike the C_2H_5 fragment, about half of the m/z 27.023 (C_2H_3) peak population shifts to 28.026 ($^{13}\text{CCH}_3$) in the spectra of $[1,2\text{-}^{13}\text{C}] - \text{Glu} + \text{H}^+$ and $[4\text{-}^{13}\text{C}] - \text{Glu} + \text{H}^+$ (Figure 2b and d). This m/z 27.023 (C_2H_3) peak shifts completely to 28.026 ($^{13}\text{CCH}_3$) in the spectrum of $[3\text{-}^{13}\text{C}] -$

$\text{Glu} + \text{H}^+$ (Figure 2c). Therefore, the carbons in this fragment mixture are C2, C3, and C3, C4. The 3,4- C_2H_3 and the 2- CH_4N fragments could originate from the m/z 56 ($\text{C}_3\text{H}_6\text{N}$) or m/z 84 ($\text{C}_4\text{H}_6\text{NO}$) fragments, whereas the 2,3- C_2H_3 and the 4- CH_4N fragments could be another pair of competing products through a rearrangement pathway. The compositions of these small fragments provide information about the origins of the carbons, and pathways to form them, as discussed below.

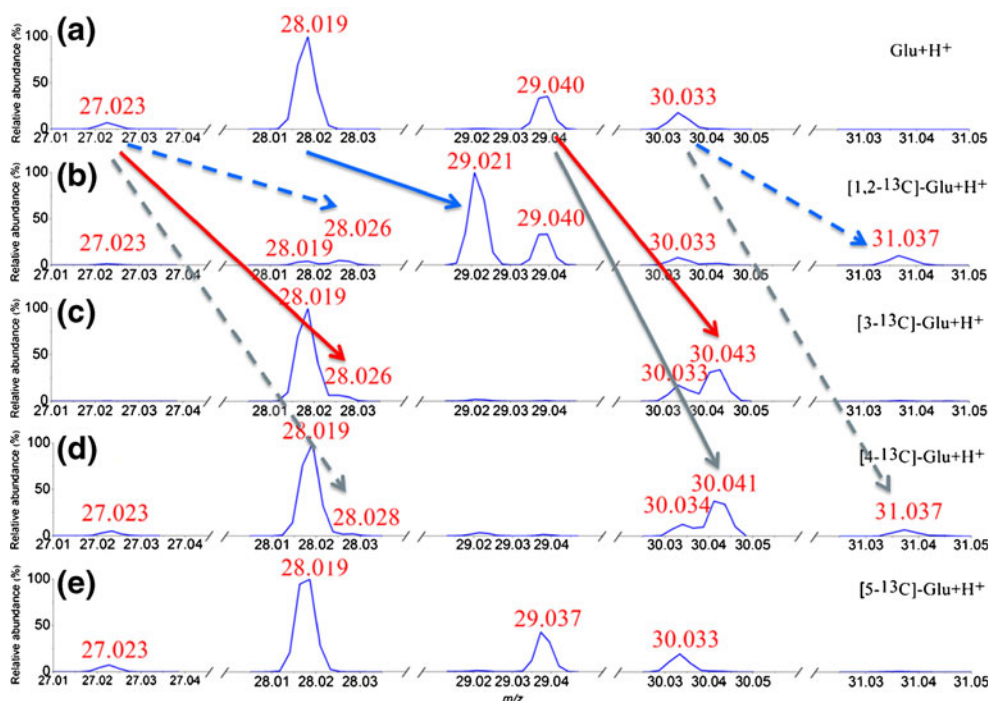


Figure 2. Low m/z fragments in MS^2 of Glu and isotopically-labeled Glu obtained on the Q-TOF instrument at 15 eV CE. (a) Glu + H^+ (m/z 148); (b) $[1,2\text{-}^{13}\text{C}] - \text{Glu} + \text{H}^+$ (m/z 150); (c) $[3\text{-}^{13}\text{C}] - \text{Glu} + \text{H}^+$ (m/z 149); (d) $[4\text{-}^{13}\text{C}] - \text{Glu} + \text{H}^+$ (m/z 149); (e) $[5\text{-}^{13}\text{C}] - \text{Glu} + \text{H}^+$ (m/z 149). The arrows show shifts of the peaks with the labeled compounds (blue for $[1,2\text{-}^{13}\text{C}] - \text{Glu} + \text{H}^+$, red for $[3\text{-}^{13}\text{C}] - \text{Glu} + \text{H}^+$ and grey for $[4\text{-}^{13}\text{C}] - \text{Glu} + \text{H}^+$). Dash-line arrows indicate that only part of the peak population shifts. Actually measured m/z values are indicated

Dissociation Pathways and Substructures of Protonated Glu

Energy resolved mass spectrometry (ERMS) curves of the precursor $\text{Glu} + \text{H}^+$ (m/z 148 MS^2) and its m/z 130 and 102 fragments (MS^3) are shown in Figure 3 to reveal the relative energetics for dissociation pathways of $\text{Glu} + \text{H}^+$. Both the m/z 130 and 102 ions are formed directly from $\text{Glu} + \text{H}^+$ ion at m/z 148 (Figure 3a). The curve of the m/z 102 fragment runs almost parallel with the m/z 130 fragment, albeit with a slightly higher energy. ERMS plots of the m/z 130 fragment (Figure 3c), confirmed that dissociation from m/z 130 to form the m/z 102 fragment is only a minor pathway. The comparison between the dissociation curves of $[\text{Glu} + \text{H}]^+$, the 130 Da and 102 Da fragments, (Figure 3a, c, and e) indicates that the major pathway to form the 102 Da fragment is from the molecular ion. In general, the dissociation pattern of the 102 Da fragment is similar to that of the $\text{Glu} + \text{H}^+$ and 130 Da (Figure 3b, d, and f). The m/z 84 fragment is the major fragmentation product of the m/z 130 and 102 ions (Figure 3c and e). This m/z 84 fragment

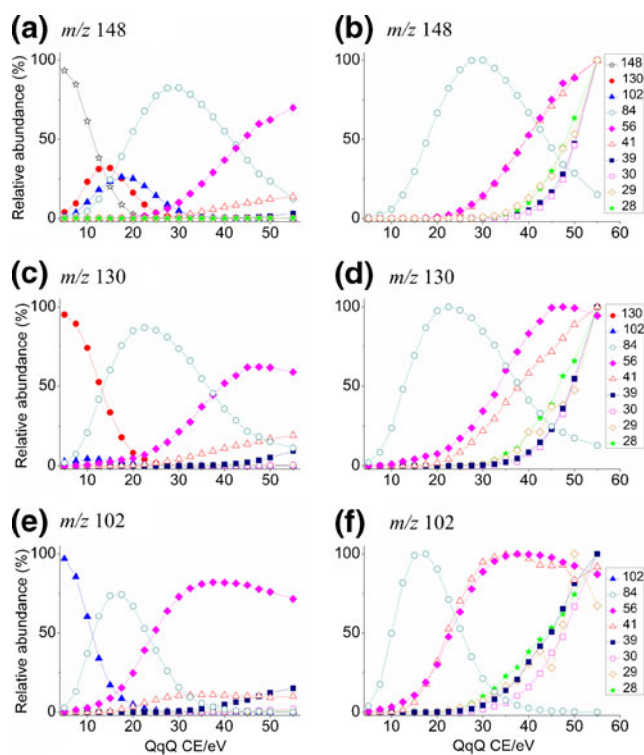


Figure 3. ERMS of dissociation of $\text{Glu} + \text{H}^+$ (m/z 148, MS^2), the m/z 130 fragment (MS^3), and the m/z 102 fragment (MS^3) in a QqQ. **(a)** ERMS of $\text{Glu} + \text{H}^+$. **(b)** Normalized ERMS of low m/z fragments ($\leq m/z$ 84) of $\text{Glu} + \text{H}^+$. Each fragment is normalized to its own maximum; **(c)** ERMS of m/z 130 fragment; **(d)** Normalized ERMS of low m/z fragments ($\leq m/z$ 84) of m/z 130 fragment. **(e)** ERMS of the m/z 102 fragment; **(f)** Normalized ERMS of low m/z fragments ($\leq m/z$ 84) of the m/z 102 fragment. Each fragment is normalized to its own maximum

further dissociates to m/z 56 and 41 fragments at ~ 30 eV and to smaller fragments at ~ 40 eV. The pathways leading to large fragments, in particular from m/z 148 to 102 and from m/z 130 to 102 were previously reported and discussed by Harrison [22, 23].

The m/z 102 fragment has two proposed structures [22]. One is linear and the other is a ring (Scheme 1). The MS^2 spectrum of protonated Glu dimethyl ester provides a clue about the structure of the Glu m/z 102 fragment (Figure S-1). A m/z 116 peak which is the methylated analog of the m/z 102 fragment was observed. Because the carboxylic acid group is still methylated, no ring is likely to be formed. Therefore, the m/z 116 is linear and, thus, a linear structure may prevail also with the Glu m/z 102 peak.

To further explore the structures of the larger fragments of $\text{Glu} + \text{H}^+$, gas-phase ammonia HDX and IM-MS were employed. The gas-phase HDX experiment shows that the m/z 84 fragment has at least three exchangeable hydrogens (Figure 4a, b), which does not fit any of the structures previously proposed [10, 11, 22–24]. This result could be explained with some linear, rearranged structures for the m/z 84 fragment. The IM drift times of the m/z 148, 130, and 84 peaks obtained in MS^2 analysis of $\text{Glu} + \text{H}^+$ at CE of 15 eV (Figure 4c–e) show that the m/z 84 peak is much broader and tailing than the other two, suggesting more than one structure in the m/z 84 fragment as proposed by Harrison [22, 23]. Further study is required to reveal the structures and pathways involving the m/z 84 fragment.

The dissociation pathway map of $\text{Glu} + \text{H}^+$ is shown in Scheme 1, now extended to low m/z fragments. The pathways to form fragments $\geq m/z$ 84 were discussed previously. At higher CE (40 eV), the m/z 84 fragment dissociates to m/z 56 [10, 11, 21] and m/z 41 fragments. These fragments further dissociate to low abundance, smaller fragments (m/z 39, 30, 29, 28, and 27) at a CE of 55 eV. The m/z 39 fragment can be formed from the m/z 41 or 56 fragments. The m/z 29 fragment does not originate from either of the fragments, m/z 41 or 39, because the m/z 29 fragment is pure 3,4- C_2H_5 , where 2,3- C_2H_5 is not observed. Because the m/z 41 and m/z 39 fragments are symmetrical, if they dissociate to the m/z 29 fragment, the 2,3- C_2H_5 should exist too. In summary, the m/z 29 fragment originated from the m/z 56 fragment, or possibly directly dissociated from the m/z 84 fragment.

The m/z 28 fragment is 2- CH_2N , as discussed before in Figure 2. This fragment and the m/z 29 fragment (3,4- C_2H_5) may be charge-competing products from the m/z 56 fragment, depending on where the proton is attached. The possibility that this fragment is directly dissociated from the m/z 84 fragment cannot be excluded. In contrast to these two fragments, the m/z 27 and 30 fragments are mixtures and there is more than one pathway to form them. Both fragments could originate from the m/z 84 or m/z 56 fragments. Because m/z 27 is a mixture of 2,3- C_2H_3 and 3,4- C_2H_3 , it may also originate from the m/z 41 and 39 fragments.

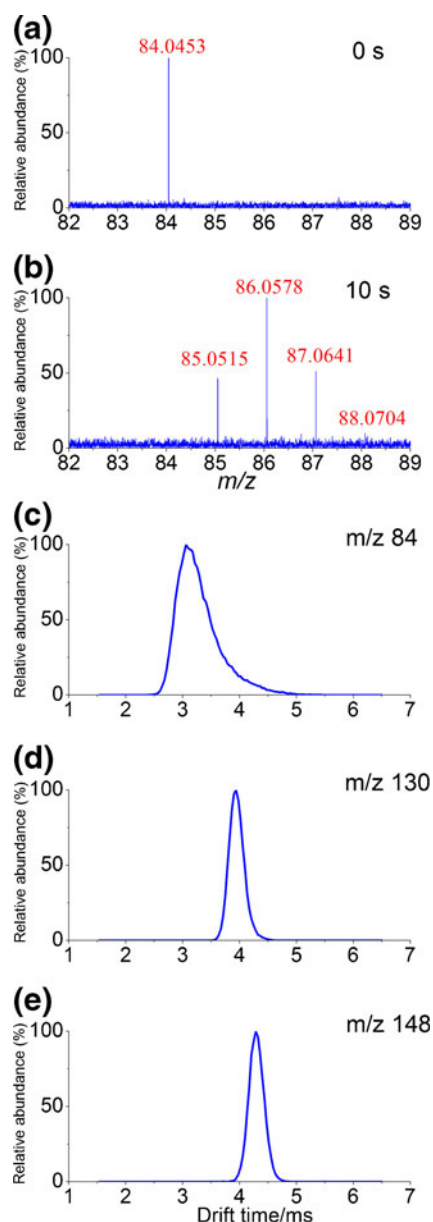


Figure 4. FTICR gas-phase HDX and IM-MS measurements. **(a,b)** FTICR gas-phase HDX of the m/z 84 fragment at 0 and 10 s **(c–e)** ion mobility drift times of m/z 148, 130, and 84 peaks in the MS^2 spectrum of Glu + H^+ at a 10 eV CE performed on Synapt G2 Q-TOF-IM-MS. The drift time peak of m/z 84 is tailing and much wider than those of the m/z 148 and 130, suggesting more than one isomer exists in the m/z 84 fragment

Low m/z Fragments of Other Amino Acids

MS^2 fragmentation patterns of protonated Gln, Pro and Ala were explored by QqQ and Q-TOF and compared with those of protonated Glu to elucidate general rules for the low m/z fragments of similar amino acids. Protonated Glu and Gln have the same medium-to-low mass ($\leq m/z$ 84) fragmentation pattern (Figure 5a–d, Table 2, and Figure S-2). To

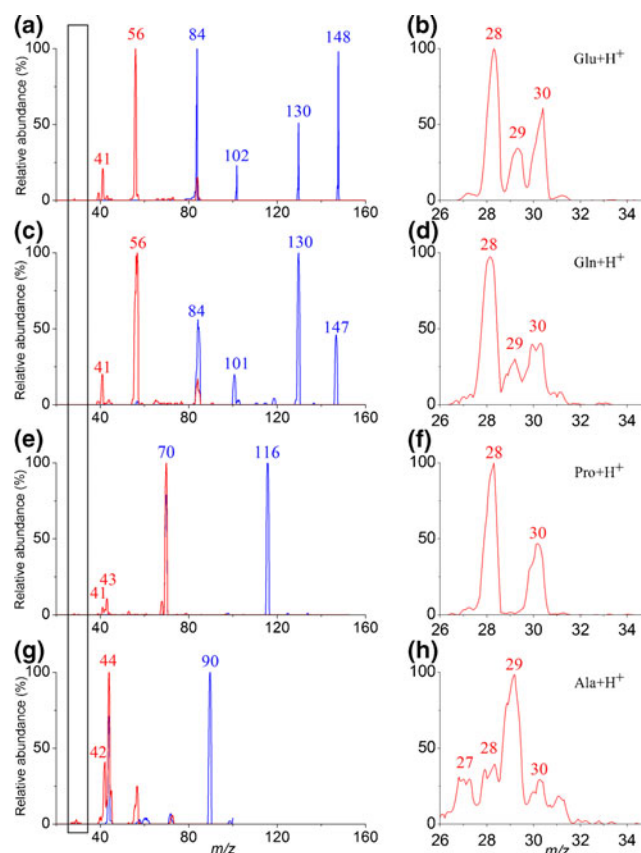


Figure 5. MS^2 of protonated Glu, Gln, Pro, and Ala performed on a QqQ in the product ion scan mode. **(a)** Glu + H^+ (m/z 148); **(c)** Gln + H^+ (m/z 147); **(e)** Pro + H^+ (m/z 116); **(g)** Ala + H^+ (m/z 90). On the left **(a, c, e, and g)** superimposed spectra are shown; **a, c, and e** are obtained at a CE of 15 eV (blue) and 55 eV (red); **g** is obtained at a CE of 13 eV (blue) and 65 eV (red). On the right **(b, d, f, and h)**, blow-ups of the low m/z region (m/z 26–35, region in rectangle, CE 55 eV for **b, d, and f**, CE 65 eV for **h**) are shown by magnifying 30 to 100 times. The spectra are normalized to the highest peak in each m/z range

distinguish, identify, and eventually quantify each labeled carbon in protonated Glu and Gln, specific fragments should be monitored. Table 2 summarizes the origins of the carbons in the low m/z fragments. Carbon identification is as follows; by comparing the shifts of the precursor and m/z 84 fragment in isotopically-labeled protonated Glu and Gln, C1 can be monitored. Similarly, the shifts of the m/z 84 and 56 fragments can be utilized to track C5. The shift of the m/z 28 fragment can be used to monitor C2 and the m/z 31 peak (shifted from 30) can be used to track C2 and C4. Because C2 can be monitored based on the m/z 28 fragment, C4 can also be tracked based on this m/z 31 peak. If C1, C2, C4, and C5 are monitored, C3 can also be deduced based on the information of the precursor and other carbons. This knowledge of the low m/z fragments is necessary to monitor each isotopically-labeled carbon in protonated Glu and Gln.

Table 2. Origins of carbons in low *m/z* fragments of protonated Glu, Gln, Pro, and Ala

<i>m/z</i>	Proposed formula	Glu	Gln	Pro	Ala
56	C ₃ H ₆ N	2,3,4-C	2,3,4-C	-	-
53	C ₄ H ₅	-	-	2,3,4,5-C	-
44	C ₂ H ₆ N	-	-	2,3-C and 3,4-C 4,5-C ^a	2,3-C
43	C ₃ H ₇	-	-	2,3,4-C ^a and 3,4,5-C ^a	-
42	C ₂ H ₄ N	-	-	2,3-C	2,3-C
41	C ₃ H ₅	2,3,4-C	2,3,4-C	2,3,4-C ^a and 3,4,5-C ^a	-
39	C ₃ H ₃	2,3,4-C	2,3,4-C	-	-
30	CH ₄ N	2-C and 4-C	2-C and 4-C	2-C and 5-C 4-C 3-C ^a	-
29	C ₂ H ₅	3,4-C	3,4-C	3,4-C ^a	-
29	CH ₃ N	-	-	-	2-C
28	CH ₂ N	2-C	2-C	2-C and 5-C 4-C 3-C ^a	2-C ^b
27	C ₂ H ₃	2,3-C and 3,4-C	2,3-C and 3,4-C	2,3-C and 3,4-C 4,5-C ^a	2,3-C

^a Origins of carbons 3,4,5 are not validated.

^b Not confirmed whether it is a pure origin.

In protonated Pro, the *m/z* 41 (C₃H₅), 30 (CH₄N), and 28 (CH₂N) fragments common to Glu and Gln, are also observed (Figure 5e, f, Table 2, and Figure S-3). The formulae of these fragments are similarly confirmed by isotopically-labeled samples (Figure S-3) and the accurate masses measured by Q-TOF (data not shown). However, the *m/z* 29 (C₂H₅) peak of Pro is very low in intensity relative to that of the *m/z* 28 and 30 fragments, supporting our previous suggestion that this ion is not originating from the *m/z* 41 fragment. In the *m/z* 84 fragment of Glu, there is an oxygen on the C5, therefore C5 is likely to dissociate as 5-CO. However, the *m/z* 70 fragment in protonated Pro (Figure 5e) contains no oxygen and C5 is not as easy to dissociate as in the *m/z* 84 in Glu. This is one of the reasons that it is more difficult to form the *m/z* 29 (C₂H₅) fragment containing C3 and C4. Owing to the lack of appropriate isotopically-labeled Pro standards, the origins of C3, C4 and C5 in Pro fragments were not confirmed in this study.

Protonated Ala has two dominant fragments in CID MS² (Figure 5g, h) – *m/z* 44 and 29 fragments. The *m/z* 44 peak shifts up by one Da in the [¹⁵N] – Ala, [2-¹³C] – Ala and [3-¹³C] – Ala (Figure S-4 c, g, and i) indicating that this peak contains nitrogen, C2 and C3, respectively. The formula of this *m/z* 44 peak is therefore 2,3-C₂H₆N, which is the result of losing the carboxylic acid group from the precursor. Unlike the other three amino acids, the *m/z* 29 peak in protonated Ala is not C₂H₅. This peak shifts up by only one Da in [¹⁵N] – Ala and [2-¹³C] – Ala (Figure S-4d and S-4h) suggesting the formula to be 2-CH₃N. This peak is the only radical ion fragment observed in this study among all nitrogen containing fragments. The *m/z* 27 peak shifts to *m/z* 28 in [2-¹³C] – Ala, [3-¹³C] – Ala (Figure S-4h and S-4j). Thus the *m/z* 27 peak is the same as that observed in the other amino acids (2,3-C₂H₃).

In summary, backbone fragments containing nitrogen and C2 are the same in the four amino acids studied in this research. The *m/z* 28 fragment in protonated Glu, Gln and Pro and the *m/z* 29 fragment in Ala can be used to monitor metabolism of ¹³C carbons at position 2 in these amino acids (Table 2).

Methylation of Glu and Gln

Depending on the amount of labeling, the nominal molecular weight (MW) of protonated, isotopically-labeled Gln may be the same as that of unlabeled protonated Glu or protonated, isotopically-labeled Glu. For example, the MW of protonated, doubly ¹³C labeled Gln, is 149 which is the same as the MW of protonated, singly ¹³C carbon labeled Glu. This mass overlap should be addressed when samples from mosquitoes or other organisms are analyzed for quantification of each carbon in isotopically-labeled amino acids. It is noted that liquid chromatography separation of Glu and Gln is also challenging and usually involves ion pairing. Derivatization of the carboxylic acid groups of Glu and Gln eliminates this interference because these two amino acids have a different number of acidic sites. Therefore, with derivatized Gln and Glu, the mass of protonated, isotopically-labeled Gln will not overlap with protonated Glu or protonated, isotopically-labeled Glu. However, the derivatizing group may form additional low *m/z* fragments in CID MS² and interfere with the analysis of the low *m/z* fragments of the amino acids. Also, derivatization may change the dissociation pathways of the “native” amino acids.

We found that methylation of the carboxylic acids is a specifically suitable way to derivatize Glu and Gln to avoid *m/z* overlapping. Trimethylsilyldiazomethane is used to methylate carboxylic acid groups under mild conditions [25] in this research. The *m/z* value of the protonated, carboxylic acids-methylated Glu is 176 and that of the protonated, carboxylic acid-methylated Gln is 161. Figure S-1 shows the fragments of the protonated dimethylated Glu. The fragments $\leq m/z$ 84 are the same as those of the underivatized protonated Glu. As a result, the derivatization does not interfere with the analysis of the low *m/z* fragments of the amino acids. Thus, methylation can be used to eliminate cross *m/z* interference of isotopically-labeled Gln and Glu or isotopically-labeled Glu, in biological samples.

Conclusions

The characterization of the fragmentation pattern of protonated Glu, Gln, Pro and Ala is extended here to fragments as low as m/z 27. The low m/z fragments are identified and dissociation pathways to form them are proposed. This knowledge is used to develop a new approach to distinguish each ¹³C-labeled carbon in the above amino acids, and potentially for more amino acids, by CID MS². The m/z 28 fragment containing nitrogen and C2 is common to protonated Glu, Gln and Pro. A similar m/z 29 fragment with C2 and nitrogen is also observed in protonated Ala. These are potential fragments to monitor C2 in the amino acids by multiple reaction monitoring (MRM). The m/z 30 fragment in protonated Glu and Gln is a mixture of 2-CH₄N and 4-CH₄N, suggesting more than one pathway to form it and one of these pathways may involve rearrangement. This fragment can be used to monitor C2 and C4. The m/z 29 and 27 fragments in protonated Glu and Gln have different carbon origins, indicating they originate from different pathways. The above carbon origins may also be fit for other amino acids.

Methylation of carboxylic acids is a specifically suitable way to further separate the MWs of Glu and Gln to avoid MW overlapping, without changing or interfering with the low m/z fragments. Although the intensity of the low m/z peaks is much weaker than the abundant high m/z fragments, by using MRM, the sensitivity can be improved to be compatible with typical levels in biological samples. The suggested MRM approach will be tested in our laboratory to monitor the incorporation of ¹³C from ¹³C-glucose into Glu, Gln, Pro and Ala in *A. aegypti* mosquitoes.

Acknowledgments

The authors thank Yang Song for her contribution in the early stages of this work, Mowei Zhou for his help on G2 Q-TOF, and George Tsapralis and Yelena Feinstein for access to the AB/SCIEX 3000 QqQ and AB/SCIEX 4000 QTRAP mass spectrometers at the Arizona Proteomics Consortium, The University of Arizona. The AB/SCIEX 4000 QTRAP mass spectrometer was provided by NIH/NCRR Grant 1S10RR022384-01. The authors are also grateful to Dr. Yayoi Hongo (RIKEN, Wako, Japan) and David R. Bush (The University of Arizona) for fruitful discussions, and Dr. Kanamatsu (Soka University, Tokyo, Japan) and Dr. Takatori (Meiji Pharmaceutical University, Tokyo, Japan) for kindly providing [4-¹³C]-Gln and [4-¹³C]-Glu, respectively, which are not commercially available. This work was financially supported by NIH/NIAID Grant R01AI088092 (to PYS).

References

1. Wiechert, W.: ¹³C metabolic flux analysis. *Metab. Eng.* **3**, 195–206 (2001)

2. Zamboni, N.: ¹³C metabolic flux analysis in complex systems. *Curr. Opin. Biotechnol.* **22**, 103–108 (2011)
3. Wiechert, W., Mollney, M., Petersen, S., de Graaf, A.A.: A universal framework for ¹³C metabolic flux analysis. *Metab. Eng.* **3**, 265–283 (2001)
4. Weitzel, M., Wiechert, W., Noh, K.: The topology of metabolic isotope labeling networks. *BMC Bioinf.* **8**, 315 (2007)
5. Rantanen, A., Rousu, J., Jouhten, P., Zamboni, N., Maaheimo, H., Ukkonen, E.: An analytic and systematic framework for estimating metabolic flux ratios from ¹³C tracer experiments. *BMC Bioinf.* **9**, 266 (2008)
6. Scaraffia, P.Y., Zhang, Q.F., Wysocki, V.H., Isoe, J., Wells, M.A.: Analysis of whole body ammonia metabolism in *Aedes aegypti* using [¹⁵N]-labeled compounds and mass spectrometry. *Insect Biochem. Mol. Biol.* **36**, 614–622 (2006)
7. Scaraffia, P.Y., Tan, G., Isoe, J., Wysocki, V.H., Wells, M.A., Miesfeld, R.L.: Discovery of an alternate metabolic pathway for urea synthesis in adult *Aedes aegypti* mosquitoes. *Proc. Natl. Acad. Sci. U.S.A.* **105**, 518–523 (2008)
8. Scaraffia, P.Y., Zhang, Q.F., Thorson, K., Wysocki, V.H., Miesfeld, R.L.: Differential ammonia metabolism in *Aedes aegypti* fat body and midgut tissues. *J. Insect Physiol.* **56**, 1040–1049 (2010)
9. Bush, D.R., Wysocki, V.H., Scaraffia, P.Y.: Study of fragmentation of arginine isobutyl ester applied to arginine quantification of *Aedes aegypti* mosquito excreta. *J. Mass Spectrom.* **47**, 1364–1371 (2012)
10. Pingitore, F., Tang, Y., Kruppa, G.H., Keasling, J.D.: Analysis of amino acid isotopomers using FT-ICR MS. *Anal. Chem.* **79**, 2483–2490 (2007)
11. Tang, Y., Pingitore, F., Mukhopadhyay, A., Phan, R., Hazen, T.C., Keasling, J.D.: Pathway confirmation and flux analysis of central metabolic pathways in *Desulfovibrio vulgaris* Hildenborough using gas chromatography-mass spectrometry and Fourier transform-ion cyclotron resonance mass spectrometry. *J. Bacteriol.* **189**, 940–949 (2007)
12. Jiang, W., Wysocki, V.H., Dodds, E.D., Miesfeld, R.L., Scaraffia, P.Y.: Differentiation and quantification of C1 and C2 ¹³C-labeled glucose by tandem mass spectrometry. *Anal. Biochem.* **404**, 40–44 (2010)
13. Szyperki, T., Glaser, R.W., Hochuli, M., Fiaux, J., Sauer, U., Bailey, J.E., Wuthrich, K.: Bioreaction network topology and metabolic flux ratio analysis by biosynthetic fractional ¹³C labeling and two-dimensional NMR spectroscopy. *Metab. Eng.* **1**, 189–197 (1999)
14. de Graaf, A.A., Mahle, M., Mollney, M., Wiechert, W., Stahmann, P., Sahm, H.: Determination of full ¹³C isotopomer distributions for metabolic flux analysis using heteronuclear spin echo difference NMR spectroscopy. *J. Biotechnol.* **77**, 25–35 (2000)
15. Wittmann, C.: Metabolic flux analysis using mass spectrometry. *Adv. Biochem. Eng. Biotechnol.* **74**, 39–64 (2002)
16. Jeffrey, F.M.H., Roach, J.S., Storey, C.J., Sherry, A.D., Malloy, C.R.: ¹³C isotopomer analysis of glutamate by tandem mass spectrometry. *Anal. Biochem.* **300**, 192–205 (2002)
17. Peng, L.F., Arauzo-Bravo, M.J., Shimizu, K.: Metabolic flux analysis for a *ppc* mutant *Escherichia coli* based on ¹³C-labeling experiments together with enzyme activity assays and intracellular metabolite measurements. *Fems. Microbiol. Lett.* **235**, 17–23 (2004)
18. Shimizu, K.: Metabolic flux analysis based on ¹³C-labeling experiments and integration of the information with gene and protein expression patterns. *Adv. Biochem. Eng. Biotechnol.* **91**, 1–49 (2004)
19. Wittmann, C.: Fluxome analysis using GC-MS. *Microb. Cell Fact.* **6**, 6 (2007)
20. Kamleh, M.A., Dow, J.A., Watson, D.G.: Applications of mass spectrometry in metabolomic studies of animal model and invertebrate systems. *Brief. Funct. Genomics Proteomics.* **8**, 28–48 (2009)
21. Piraud, M., Vianey-Saban, C., Petritis, K., Elfakir, C., Steghens, J.P., Morla, A., Bouchu, D.: ESI-MS/MS analysis of underivatized amino acids: a new tool for the diagnosis of inherited disorders of amino acid metabolism. Fragmentation study of 79 molecules of biological interest in positive and negative ionisation mode. *Rapid Commun. Mass Spectrom.* **17**, 1297–1311 (2003)
22. Harrison, A.G.: Ion chemistry of protonated glutamic acid derivatives. *Int. J. Mass Spectrom.* **210**, 361–370 (2001)
23. Harrison, A.G.: Fragmentation reactions of protonated peptides containing glutamine or glutamic acid. *J. Mass Spectrom.* **38**, 174–187 (2003)
24. Harrison, A.G.: To b or not to b: the ongoing saga of peptide b ions. *Mass Spectrom. Rev.* **28**, 640–654 (2009)
25. Presser, A., Hufner, A.: Trimethylsilyldiazomethane - A mild and efficient reagent for the methylation of carboxylic acids and alcohols in natural products. *Monatsh. Chem.* **135**, 1015–1022 (2004)